

# Testing and applicability of the UPC-ZEBRA interferometer as a phasing system in segmented-mirror telescopes

Agustí Pintó, Ferran Laguarda, Roger Artigas, and Cristina Cadevall

In segmented-mirror telescopes, wave-front discontinuities caused by segment misalignment are a major problem because they severely degrade optical performance. While angular misalignments are usually measured with deflectometric wave-front sensors (e.g., Shack–Hartmann sensors), a number of techniques have been proposed for the measurement of vertical discontinuities (pistons). In earlier papers we presented an instrument called UPC-ZEBRA that uses a novel interferometric technique to measure piston error during the daytime with an uncertainty of 5 nm within a 30- $\mu$ m range. Here we present the most representative results obtained during the testing stage and a detailed analysis of error sources. The main modifications to be introduced for the instrument's use as a phasing calibration system are also outlined. © 2004 Optical Society of America

*OCIS codes:* 110.6770, 350.1260, 120.3180, 120.3930.

## 1. Introduction

Segmented mirrors and adaptive-optics (AO) techniques are fundamental to the design of ground-based telescopes both today and in the future. It is well known that proper segment positioning is crucial to both near-diffraction-limit telescope performance in the infrared region and the proper operation of AO-based instruments. The construction of the Keck telescopes<sup>1</sup> demonstrated the viability of the segmented design, and the phasing techniques used<sup>2–5</sup> provided valuable information on features that would be desirable in future phasing systems. An example of such features can be found in the conceptual design of the Gran Telescopio Canarias (GTC),<sup>6</sup> in which special interest is shown for a daytime phasing system that has nanometric accuracy and that requires no interaction with the mirror segments.

In earlier papers<sup>7–8</sup> we presented the UPC-ZEBRA interferometer, designed specifically to measure rel-

ative segment misalignment locally at each intersegment during the daytime. The instrument is based on a high-aperture Michelson interferometer that uses a novel optical-fiber illumination technique.

To obtain the desired piston measurement between a given pair of segments, we send the measurement beam to the contact region between the segments (the intersegment). Instead of using an internal reference mirror, we send the reference beam to a region of one of the segments that was situated as close as possible to the measurement region (see Fig. 1). This provides the interferometer with a high degree of both wave-front matching and vibration insensitivity. An afocal system placed on the observation arm allows the observation of the interference pattern and, at the same time, the imaging of a 45.3-mm-by-34-mm area of the segments on the CCD array. Such a large observation area, attained through the use of high-aperture optics (50 mm in diameter), is necessary to minimize the effects of segment figure errors (which are expected to be large near the edges) on piston measurements.

The measurement principle is based on a novel illumination technique that combines the light of different bandwidths by use of an optical fiber.<sup>8</sup> A composite spectrum, comprising a narrowband component over a broadband background, is obtained (see Fig. 2). When such an illumination spectrum is used in an interferometer, the resulting interferograms are the sum of narrowband and broadband

---

The authors are with the Center for Sensors, Instruments and Systems Development (CD6), Universitat Politècnica de Catalunya (UPC) Rambla Sant Nebridi, 10, E-08222 Terrassa, Spain. F. Laguarda's e-mail address is laguarda@oo.upc.es.

Received 5 March 2003; revised manuscript received 20 June 2003; accepted 8 October 2003.

0003-6935/04/051091-06\$15.00/0

© 2004 Optical Society of America

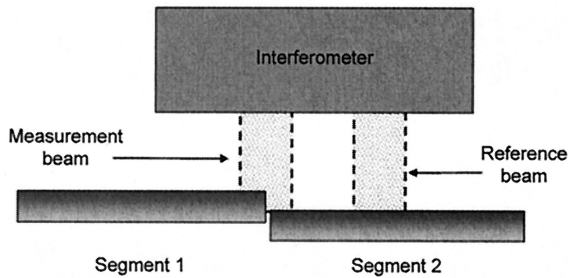


Fig. 1. UPC-ZEBRA interferometer positioned over an intersegment.

fringe patterns. Therefore the result is basically a monochromatic interference pattern with a few fringes, those closer to an optical path difference (OPD) of zero, having a higher contrast (see Section 3). An absolute reference is thus introduced into a monochromatic interference pattern, allowing us to unambiguously remove the  $\lambda/2$  indetermination.

A suite of processing algorithms has been developed to extract segment misalignment data from a single composite interferogram.<sup>8</sup>

In this paper we present the most representative results obtained during the testing stage of the UPC-ZEBRA interferometer at the Center for Sensors, Instruments and Systems Development (CD6) laboratory and at the GTC test workbench, where the final test was carried out. Section 2 contains a description of the laboratory and GTC test workbench setups. Section 3 presents a selection of the most representative results obtained during the testing stages of the UPC-ZEBRA interferometer. This section also includes a detailed analysis of the error sources that might degrade interferometer performance. Section 4 includes a discussion on the applicability of the UPC-ZEBRA interferometer to the phasing of a segmented mirror, as well as the main

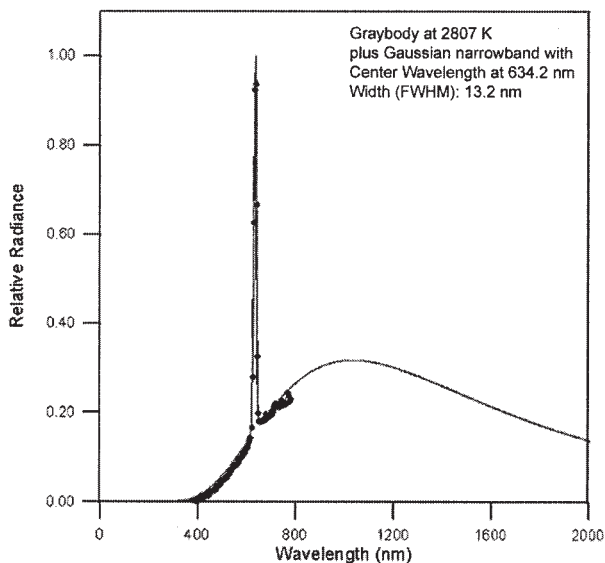


Fig. 2. Experimentally measured composite spectrum (dots) and mathematical fit (continuous curve).

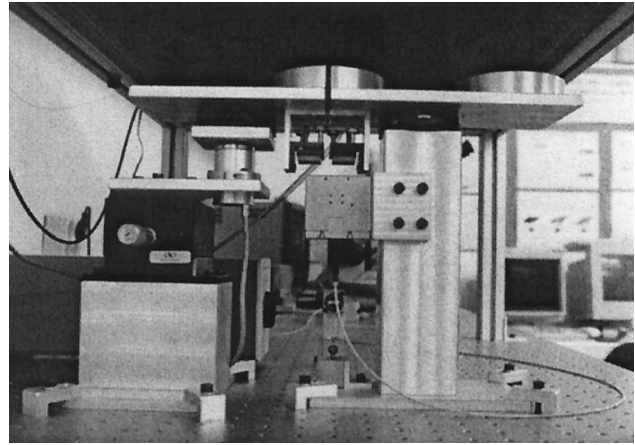


Fig. 3. Intersegment simulator: segment 1 is on the left, mounted on a manual vertical stage and a PZT; segment 2 is on the right. The bottom part of the UPC-ZEBRA interferometer is seen at the top of the figure.

modifications necessary for its use as a routine phasing calibration system. Section 5 presents the general conclusions and areas for future study.

## 2. Experimental Setup

A detailed description of the interferometer itself can be found in Refs. 7 and 8. Because the interferometer measures segment misalignment locally at each intersegment, a system for reproducing such a contact region was built in the laboratory (an intersegment simulator). This system is shown in Fig. 3.

To simulate an intersegment, we cut a mirror into two halves, each of which was mounted on a separate baseplate. Also, another mirror was mounted on one of the baseplates to simulate the reference region. Simulating segments 1 and 2 (see Fig. 1), the two baseplates were mounted on aluminum blocks that positioned them within the depth of focus of the interferometer and close to each other (1 mm). High-precision angular positioners were used to align the baseplates with the interferometer. Segment 2 was fixed, whereas segment 1 was mounted on a manual vertical positioner and a three-axis piezoelectric transducer (PZT) to introduce a controlled piston between the segments. Also, to monitor a differential piston, a commercial interferometer (Hewlett-Packard Model HP10719A) was mounted below the intersegment.

Although the mirrors we used were flat, the actual segments were off-axis sections of a hyperboloid. Predesign simulations<sup>9</sup> showed that using hyperbolic segments with the characteristics of the GTC would introduce, at worst, a  $\lambda/20$  astigmatism to the difference wave front. Because the quality of the optics used is also  $\lambda/20$ , one can conclude that the interferograms obtained at the laboratory would be identical to those obtained from a real segmented mirror.

Another intersegment simulator was built to check interferometer accuracy and stability. A one-piece flat mirror was placed in the measurement region to

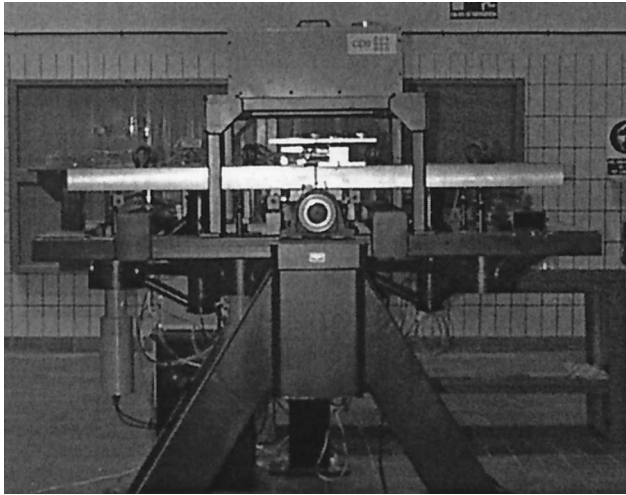


Fig. 4. UPC-ZEBRA interferometer installed on the GTC test bench.

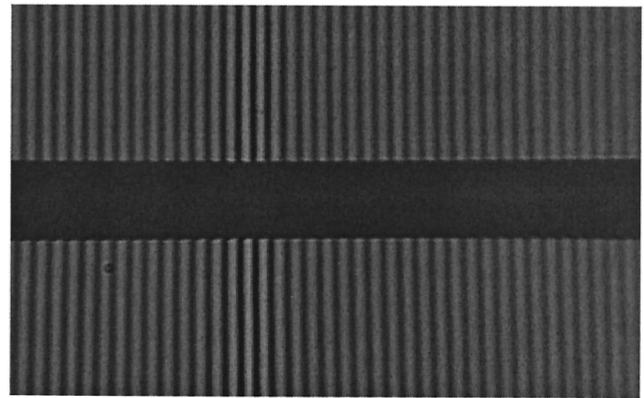
simulate the zero-piston condition of a phased intersegment simulator.

Once the laboratory tests were finished, the interferometer was taken to the facilities of Grantecan S. A. at the Instituto de Astrofísica de Canarias, where the final test was performed. A real-scale two-segment test bench was built there to test the performance of the segment actuators, the capacitive sensors, and the UPC-ZEBRA interferometer (see Fig. 4).

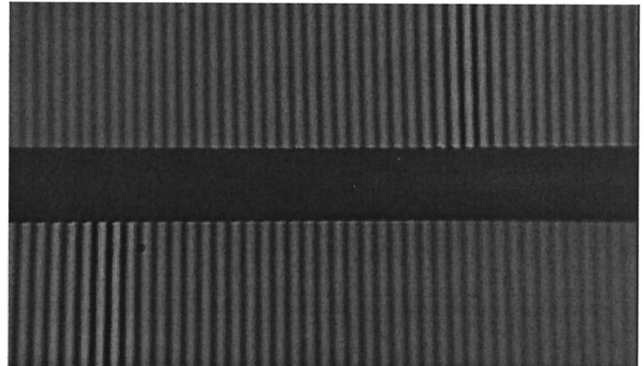
### 3. Results

A typical interferogram shows three distinct regions: segment 1 (upper subfield), the gap between the segments, and segment 2 (lower subfield), which is used as a reference. An experimental interferogram of a phased intersegment is shown in Fig. 5(a). The absence of fringe mismatching (as shown by the highest contrast fringes, which indicate zero OPD) and the similar appearance of the interferential patterns in both segments indicate that the segments are aligned. Another interferogram is shown in Fig. 5(b). The piston is apparent from the fringe mismatching. The size of the piston is calculated as the difference between the positions of the zero OPD fringes by use of the pixel scale (nanometers per pixel) extracted from the monochromatic component of the interferograms.<sup>8</sup> Angular misalignments can be measured because they affect the upper subfield interferograms: Relative segment tilt causes the fringe period to change, and relative segment tip causes the fringes to deviate from the vertical. Control software alerts the user when either tip or tilt is too high for proper piston measurement. A typical interferogram obtained in the presence of angular and piston misalignments is shown in Fig. 5(c).

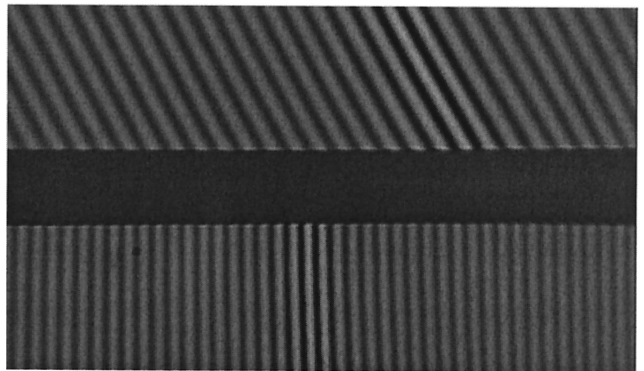
Extensive tests were carried out in the laboratory to determine the accuracy and repeatability of UPC-ZEBRA in measuring piston between segments and to identify possible error sources that could degrade the interferometer's performance.



(a)



(b)



(c)

Fig. 5. Experimental interferograms acquired (a) under phased segment conditions, (b) with 8- $\mu\text{m}$  piston, (c) with piston and angular misalignments. The measurement range was set to 12  $\mu\text{m}$ .

First, accuracy tests were carried out by use of the phased intersegment simulator. One of these tests is shown in Fig. 6. Given that the measurement region is a one-piece flat mirror, the piston measured would have ideally been 0 nm. However, this was not the case with the real measurements. The average values of zero-piston measurements were typically in the range of 3–7 nm. This must be attributed to the fact that the proper alignment conditions of the interferometer are not easily achieved. The computer algorithm that checks these conditions has a built-in margin of error that simplifies instrument operation and still provides reliable results. Higher accuracy could be obtained with a computer-



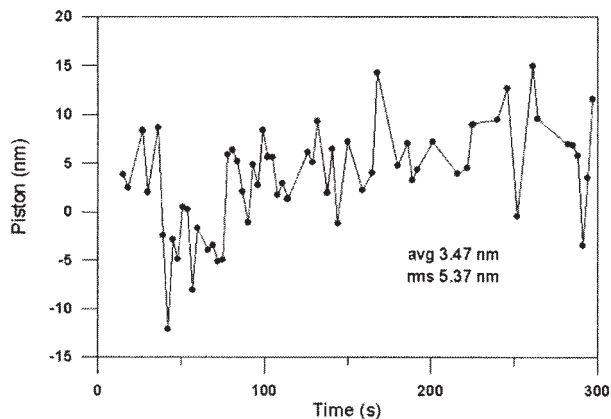


Fig. 6. Accuracy test performed with the phased intersegment simulator.

assisted interferometer alignment procedure or with improved interferogram processing algorithms, leading to the preliminary conclusion that the interferometer's accuracy depends largely on the alignment conditions.

Following these tests, UPC-ZEBRA repeatability was measured with the two-segment intersegment simulator. In these tests a set of time-series measurements were acquired for a fixed piston value. To monitor the simulation system's mechanical drift, the reference measurements provided by the external interferometer (HP10719A) were used. The root-mean-square (rms) value of the measurements provided by UPC-ZEBRA with respect to those provided by HP10719A is considered to represent the repeatability of the measurement.

In Figs. 7(a) and 7(b), several 20-s piston measurement series are plotted for two different piston measurement ranges (4 and 12  $\mu\text{m}$ ). These figures illustrate to a great extent the repeatability behavior of the interferometer. They show that interferometer repeatability is independent of the measurement range and that it has a value of 5 nm. The analysis performed during the design stages showed that fringe sampling at the CCD array would be the limiting factor for repeatability. Because radiometric calculations<sup>9</sup> showed evidence of a good signal-to-noise ratio, photon noise was not considered. However, the observed repeatability is much larger than that expected and has to be attributed to another factor. The effect of atmospheric perturbations (time-evolving refractive-index inhomogeneities) on the quality of the wave-fronts was identified as one such limiting factor.

The linearity tests were carried out last. The aim of these tests was to analyze whether the behavior of the interferometer is independent of the actual piston value. To obtain dynamic piston measurements, segment 1 was pistoned by use of the PZT in a sawtooth curve during data acquisition. The system's linearity was calculated with the data provided by the external interferometer (HP10719A) as a reference. In Fig. 8 linearity measurements are shown

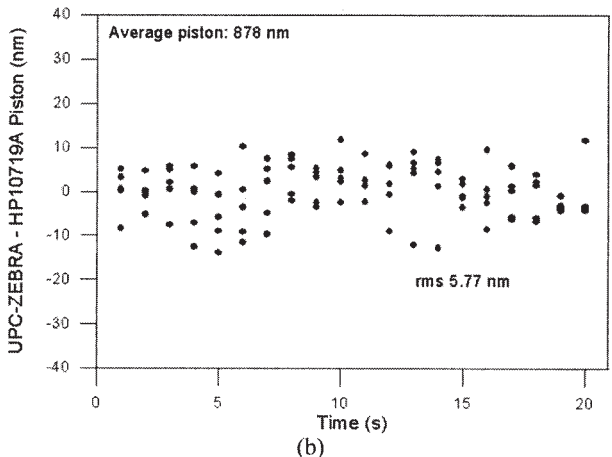
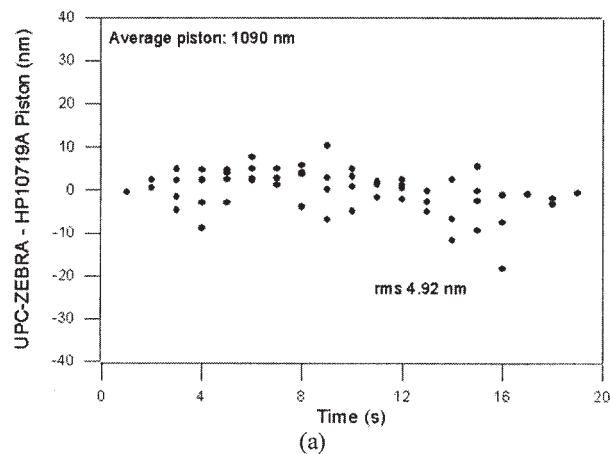


Fig. 7. Repeatability tests. The piston measurement range was set to (a) 4 and (b) 12  $\mu\text{m}$ .

for the 12- $\mu\text{m}$  measurement range. In Fig. 8(a) the piston value measured by UPC-ZEBRA is plotted against that measured by HP10719A. Near-linear behavior is observed. Residuals between UPC-ZEBRA and HP10719A measurements versus the output provided by HP10719A are plotted in Fig. 8(b), which shows that the residuals are independent of the piston and exhibit an rms fluctuation of 5 nm. The values shown in this figure match those obtained in the repeatability tests.

Although designed specifically to measure piston, UPC-ZEBRA can also measure the between-segment tip and tilt, which are usually measured with a Shack-Hartmann camera. When the tip and tilt have been removed, the piston can be measured. However, if some residual tip and tilt misalignment remains, it can be measured at the same time as the piston, to achieve better phasing.

#### 4. Applicability

The ability of the prototype UPC-ZEBRA interferometer to measure piston between two segments during daytime was successfully tested. However, a complete phasing calibration system should be able to automatically measure piston errors between all the segments of a primary mirror. In order to accom-

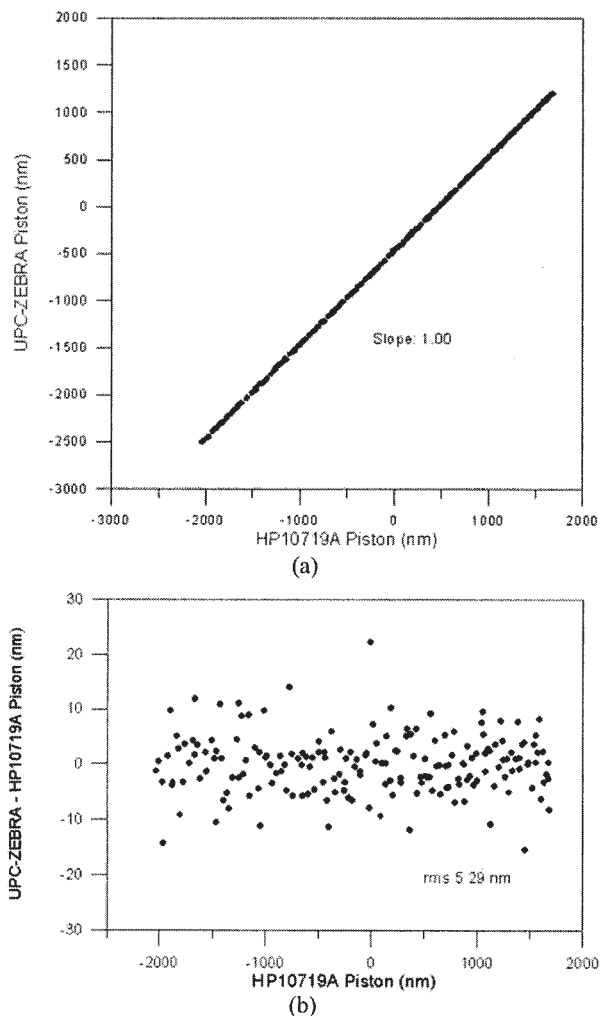


Fig. 8. Linearity test for a 12- $\mu\text{m}$  measurement range. (a) plot of UPC-ZEBRA piston versus HP10719A piston and (b) plot of residuals between UPC-ZEBRA and HP10719A pistons versus HP10719A piston.

plish this, a set of modifications and some auxiliary systems are required.

The tests carried out showed that the accuracy of the prototype was limited by the sensitivity of the processing algorithms to the alignment conditions, which proved too strict to be easily attained. Moreover, the simulations carried out during the design stages showed that system accuracy would also depend on segment figure errors (which are expected to be between 20 and 30 nm). The processing algorithms need to be modified so that they can obtain piston measurements under more lenient alignment conditions. They must also take into account the effect of segment figure errors on interferograms. The current accuracy of the prototype, which uses  $\lambda/20$  mirrors, is 3 nm, however, the ideal value would be 1 nm.

The tests also showed that repeatability was limited by the effect of atmospheric perturbations on the quality of the wave-fronts. To minimize this effect, the beams should be confined as much as possible

Table 1. UPC-ZEBRA Specifications

Specification	Value
Working distance	100 mm
Positioning tolerance	>10 mm
Mechanical stability	>1 h
Beam aperture	50 mm $\phi$
Maximum measuring range	30 $\mu\text{m}$
Repeatability	5 nm rms
Acquisition frequency	25 fps <sup>a</sup>
Separation between the reference and measurement beams	170 mm
Tip measurement range	$\pm 0.9^\circ$
Tilt measurement range	$\pm 0.05^\circ$

<sup>a</sup>fps = frames per second.

while they are traveling inside the interferometer. Moreover, a complete analysis of these perturbations inside a dome is necessary to assess their effect on repeatability. The prototype's current repeatability under laboratory conditions is 5 nm, and the goal would be to maintain this value.

Some optical redesign is also considered necessary: The aperture of the system must be increased to minimize the effect of segment figure errors on piston measurement. In addition, a lighter, more compact interferometer would be beneficial.

Two auxiliary systems are required for the interferometer to be used as a routine phasing calibration system: (1) an automatic positioning mechanism (a robotic arm) to sequentially place the interferometer in front of each of the pair of segments whose relative misalignment needs to be measured and (2) a fine alignment system to precisely and automatically align the interferometer once it has been properly positioned. A complete analysis on the admissible positioning tolerances of the interferometer has already been conducted, followed by the identification of aerial platforms as the most suitable commercially available positioning systems. However, one might expect the interferometer to oscillate with respect to the segmented mirror on a scale large enough to prevent interferometric measurements from being carried out. An active control system is necessary to compensate for these oscillations. Such a control system is currently being integrated into the prototype.

## 5. Conclusions

In this paper the results of testing the UPC-ZEBRA interferometer have been presented. The main conclusion regarding the performance of the system is that it can take daytime measurements of the between-segment piston error with a repeatability of 5-nm rms and within a range of 30  $\mu\text{m}$ . Tests have shown that the system can also measure residual tip and tilt misalignments. The phasing requirements for segmented telescopes in which AO instruments are to be used can be achieved by use of the system presented in this paper. Table 1 provides a summary of the characteristics of the interferometer.

The tests performed have shown that the accuracy of the UPC-ZEBRA interferometer is limited by the processing algorithms' sensitivity to the alignment conditions to a value in the 3–7-nm range. They have also shown that the effect of atmospheric perturbations on the wave-fronts limits the instrument's repeatability to 5 nm, irrespective of the measurement range.

The applicability of the UPC-ZEBRA interferometer as a routine phasing calibration system has also been evaluated. Some modifications have been proposed in order to overcome the limitations found in the testing stages, and two required auxiliary systems have been presented. The modifications include confining the beams inside the interferometer as much as possible to minimize the effect of atmospheric perturbations on wave fronts and revising the processing algorithms so that they can measure piston under more relaxed alignment conditions. Also, these algorithms should take into account the effect of segment figure errors on interferograms. In the applicability assessment it was pointed out that two auxiliary systems are required: (1) an automatic positioning mechanism to sequentially place the interferometer in front of each pair of segments whose relative misalignment needs to be measured and (2) a fine alignment system to precisely and automatically align the interferometer once it has been properly positioned.

The authors thank J. Arasa, C. Pizarro, and N. Tomàs for their substantial contributions to the design of the instrument. The authors also thank Grantecan S. A. and the Comisión Interministerial de Ciencia y Tecnología for providing the funds for the

development of this project. A. Pintó thanks the Department of Universities, Research and Information Society, for the PhD grant he received, which enabled him to take part in this work.

## References

1. J. Nelson, T. Mast, and S. Faber, "The design of the KECK observatory and telescope," Keck Observatory Report 90 (W. M. Keck Observatory, Kamuela, Hawaii, 1985).
2. G. Chanan, M. Troy, F. Dekens, S. Michaels, J. Nelson, T. Mast, and D. Kirkman, "Phasing the mirror segments of the Keck telescopes: the broadband phasing algorithm," *Appl. Opt.* **37**, 140–155 (1998).
3. G. Chanan, M. Troy, and E. Sirko, "Phasing the Keck telescope with out-of-focus images in the infrared," *Appl. Opt.* **38**, 704–713 (1999).
4. G. Chanan, M. Troy, and C. Ohara, "Phasing the mirror segments of the Keck telescopes: a comparison of different techniques," in *Optical Design, Materials, Fabrication, and Maintenance*, P. Dierickx, ed., *Proc. SPIE* **4003**, 188–202 (2000).
5. G. Chanan, C. Ohara, and M. Troy, "Phasing the mirror segments of the Keck telescope II: the narrow-band phasing algorithm," *Appl. Opt.* **39**, 4706–4714 (2000).
6. Grantecan Project Office, *GTC Conceptual Design* (Grantecan S.A., La Laguna, Spain, 1997).
7. C. Pizarro, J. Arasa, F. Laguarda, N. Tomàs, and A. Pintó, "Design of an interferometric system for the measurement of phasing errors in segmented mirrors," *Appl. Opt.* **41**, 4562–4570 (2002).
8. A. Pintó, F. Laguarda, R. Artigas, and C. Cadevall, "New interferometric technique for piston measurement in segmented mirrors," *J. Opt. A* **4**, S369–S375 (2002).
9. A. Pintó, "New interferometric technique for piston measurement and phasing of segmented mirrors," Ph.D. dissertation (Universitat Politècnica de Catalunya, Barcelona, Spain, 2002).